Catalysis Letters 7 (1990) 107–118

METAL EFFECTS IN THE FISCHER-TROPSCH SYNTHESIS: BOND-ORDER-CONSERVATION-MORSE-POTENTIAL APPROACH

Evgeny SHUSTOROVICH

Corporate Research Laboratories, Eastman Kodak Company, 1966 Lake Ave., Rochester, NY 14650-2001, U.S.A.

Fischer-Tropsch synthesis, heterogeneous catalysis, theoretical modeling, bond-order conservation, Morse potential, single-crystal surfaces, catalytic properties of Fe(110), Ni(111), Pt(111), Cu(111)

We have applied the BOC-MP method to theoretically analyze the metal effects in the Fischer-Tropsch (FT) synthesis by calculating the energetics of conceivable elementary steps (the relevant heats of chemisorption and the reaction activation barriers) during CO hydrogenation over the periodic series Fe(110), Ni(111), Pt(111), Cu(111). The basic steps such as dissociation of CO, hydrogenation of carbidic carbon, C–C chain growth by insertion of CH_2 versus CO into the metal-alkyl bonds, and chain termination leading to hydrocarbons (alkanes versus α-olefins) or oxygenates are discussed in detail. It is shown that the periodic trends in the ability of metal surfaces to dissociate chemical bonds and those to recombine the bonds are always opposite. In particular, we argue that metallic Fe is necessary to produce the abundance of carbidic carbon from CO but the synthesis of hydrocarbons and oxygenates can effectively proceed only on carbided Fe surfaces which resemble the less active metals such as Pt. More specifically, we project that the C–C chain growth should occur predominantly via CH_2 insertion into the metal-alkyl bond and the primary FT products should be α-olefins. These and other model projections are in agreement with experiment.

1. Introduction

The Fischer-Tropsch (FT) synthesis is the process of formation of various hydrocarbons (mostly alkanes and α-olefins) and oxygenates (principally, alcohols) that occurs during hydrogenation of CO over supported metal catalysts [1]. Since C_1 products such as CH_4 and CH_4OH can be produced on a variety of metal and nonmetal catalysts [1–3], the essence of the FT synthesis is C–C chain growth leading to higher hydrocarbons and oxygenates. The CO hydrogenation is believed to proceed by the elementary steps outlined in fig. 1, although many mechanistic details are still not resolved [1,4]. The serious aggravation here is that practical FT catalysts are never pure metals but complex combinations of metals, supports, and additives (promoters and poisons). Thus, the necessary step in elucidating the mechanisms of the FT synthesis is to separate the intrinsic metal

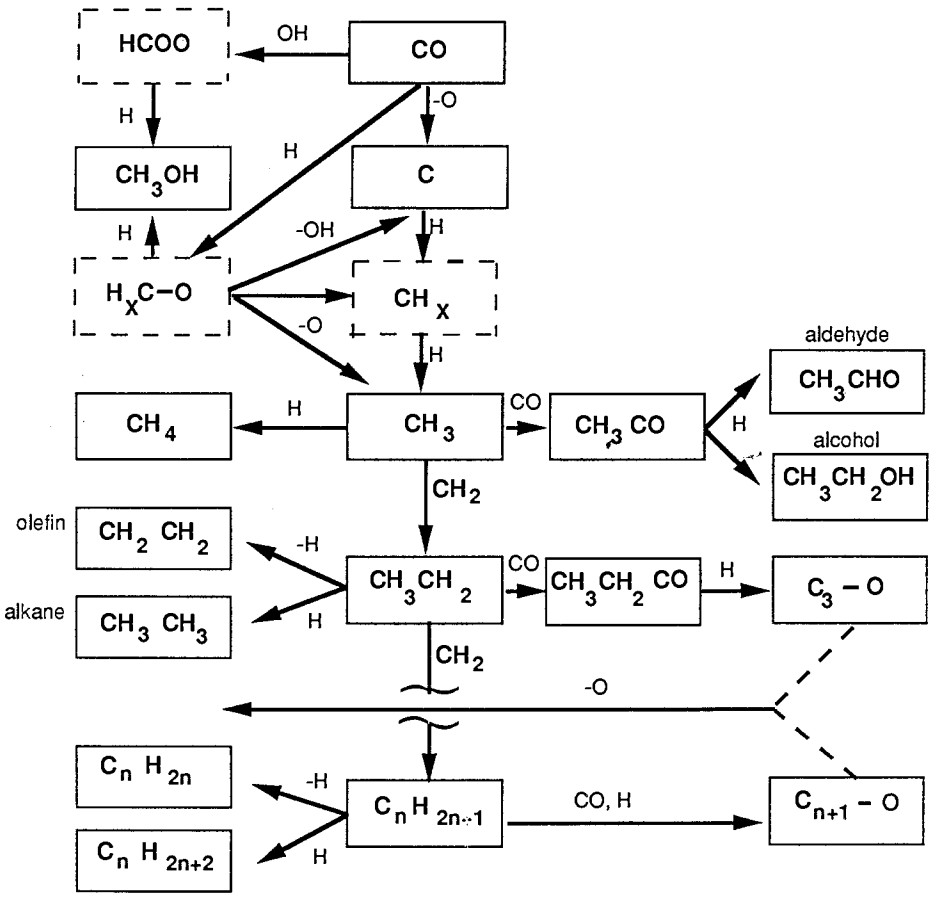

Fig. 1. Conceivable elementary reaction steps in hydrogenation of CO leading to the Fischer-Tropsch synthesis.

effects, particularly the periodic trends in the ability of metal catalysts to propagate C–C chains and to produce hydrocarbons versus oxygenates.

Arguably, this separation can be done mainly in "thought" experiments, that is, by theory. Below we will attempt a theoretical analysis of the metal effects in the FT synthesis by using our bond-order-conservation Morse-potential (BOC-MP) approach [5–7]. This analytic approach proved to be efficient in calculating reaction energetics on transition metal surfaces, namely the heats of chemisorption Q of various adsorbates and the activation barriers ΔE^* for adsorbate dissociation, recombination (including molecular insertion), and disproportionation. The text will be organized as follows. First, we will recall the BOC-MP formalism to treat the reaction energetics. Then, we will calculate the values of Q and ΔE^* for the elementary steps outlined in fig. 1, and this will be done in a periodic manner for such representative metal surfaces as Fe(110), Ni(111), Pt(111), and Cu(111). Then, based on our calculations of Q and ΔE^* for the

conceivable elementary steps of CO hydrogenation, we will project the periodic trends in the basic reactions comprising the FT synthesis, particularly CO dissociation to form carbidic carbon and its stepwise hydrogenation, C–C chain growth by insertion of CH_2 versus CO into the metal-alkyl bonds, and chain termination leading to hydrocarbons (alkanes versus olefins) or oxygenates. We will show that the periodic trends in the ability to dissociate chemical bonds and those to recombine the bonds are always opposite. We will compare our conclusions with representative experimental data and comment on the efficiency of the BOC-MP modeling.

2. BOC-MP formalism

We consider an AB molecule interacting with n metal M surface atoms to form the M_n-AB chemisorption bond. One should distinguish between weak and strong chemisorption. The weakly bound AB molecules typically have a closed electronic shell; for example, H_2, N_2, CO, NH_3, H_2O, or unpaired electrons occupying the substantially delocalized molecular orbitals, e.g., NO or O_2. The strongly bound AB molecules have unpaired electrons retaining their atomic character, such as CH, CH_2, NH, OH, or OCH_3. Analytically, the difference between the weak and strong M_n–AB bonding is reflected in the use of different effective Morse constants, Q_{0A} (for the M–A bond) and Q_A (for the M_n–A bond), respectively, which relate as

$$Q_A = Q_{0A}(2 - 1/n). \tag{1}$$

For the weak M_n–AB bonding, the simplest case corresponds to AB perpendicular to a surface with the A end down when

$$Q_{AB,n} \leqslant \frac{Q_{0A}^2}{(Q_{0A}/n) + D_{AB}} \quad \text{for } D_{AB} > \frac{n-1}{n} Q_{0A}. \tag{2}$$

For the strong M_n–AB bonding (also coordinated via A) we have

$$Q_{AB} = \frac{Q_A^2}{Q_A + D_{AB}} \tag{3}$$

which is an analog of eq. (2) for $n = 1$. For monovalent radicals AB such as CH_3 or HCO, one can expect the intermediate M_n–AB bonding, which is an average of eqs. (2) and (3), namely

$$Q_{AB} = \frac{1}{2}\left[\frac{Q_{0A}^2}{(Q_{0A}/n) + D_{AB}} + \frac{Q_A^2}{Q_A + D_{AB}}\right]. \tag{4}$$

The BOC-MP theory can similarly treat dicoordination

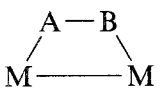

where both A and B are involved in chemisorption bonding. Here we will recall only the formula for the weak homonuclear (A = B) bonding, namely

$$Q_{A_2} = \frac{(\frac{9}{2})Q_{0A}^2}{3Q_{0A} + 8D_{A_2}} \tag{5}$$

which will be used below to calculate Q_{A_2} for ethylene C_2H_4 and acetylene C_2H_2 ($A = CH_2$ and CH, respectively).

If AB approaches a surface from the gas phase, the activation barrier $\Delta E^*_{AB,g}$ for dissociation $AB_g \rightarrow A_s + B_s$ explicitly depends on the dissociation bond energy D_{AB} and the chemisorption energies of all adsorbates; namely, the barrier can be approximated as

$$\Delta E^*_{AB,g} = \tfrac{1}{2}\left(D_{AB} + \frac{Q_A Q_B}{Q_A + Q_B} - Q_{AB} - Q_A - Q_B \right). \tag{6}$$

Since the dissociation barrier $\Delta E^*_{AB,s}$ from a chemisorbed state will be larger than $\Delta E^*_{AB,g}$ just by the amount of the molecular heat of chemisorption Q_{AB}, that is

$$\Delta E^*_{AB,s} = \Delta E^*_{AB,g} + Q_{AB} \tag{7}$$

one finally obtains

$$\Delta E^*_{AB,s} = \tfrac{1}{2}\left(D_{AB} + \frac{Q_A Q_B}{Q_A + Q_B} + Q_{AB} - Q_A - Q_B \right). \tag{8}$$

In general, for the reverse reaction of recombination, the activation barriers can be calculated from the relevant thermodynamic cycles. Specifically, for the recombination of chemisorbed A_s and B_s to chemisorbed AB_s or gas-phase AB_g, the activation barriers $\Delta E^*_{A-B,s}$ and $\Delta E^*_{A-B,g}$ may be the same or different, depending on the sign of the gas-phase dissociation barrier $\Delta E^*_{AB,g}$, namely,

$$\Delta E^*_{A-B,s} = \Delta E^*_{A-B,g} = Q_A + Q_B - D_{AB} + \Delta E^*_{AB,g} \text{ if } \Delta E^*_{AB,g} > 0 \tag{9}$$

or

$$\Delta E^*_{A-B,g} = \Delta E^*_{A-B,s} - \Delta E^*_{AB,g} = Q_A + Q_B - D_{AB} \text{ if } \Delta E^*_{AB,g} < 0. \tag{10}$$

We can also treat a variety of disproportionation reactions

$$A + BC \leftrightarrows [A \ldots B \ldots C] \leftrightarrows AB + C \tag{11}$$

that proceed without major geometric reorganization of the fragments via the transition state [A...B...C], where A may be either an atomic or molecular adsorbate and BC a diatomic or polyatomic admolecule. Arranging in eq. (11) the disproportionating species such that

$$D = D_A + D_{BC} - D_{AB} - D_C > 0 \tag{12}$$

we can treat A + BC as a quasimolecule (with the total gas-phase bond energy $D_{A+BC} = D_A + D_{BC}$ and the total heat of chemisorption $Q_{A+BC} = Q_A + Q_{BC}$), which dissociates into two fragments, AB and C (with the relevant energies D_{AB},

Q_{AB}, D_C, and Q_C). Then, the activation barrier ΔE_f^* for the forward reaction in eq. (11) may be calculated as the dissociation barrier $\Delta E^*_{(AB)C}$, which, from the gas phase, will be [cf. eq. (6)]

$$\Delta E^*_{f,g} = \Delta E^*_{(AB)C,g} = \tfrac{1}{2}\left(D + \frac{Q_{AB}Q_C}{Q_{AB}+Q_C} - Q_A - Q_{BC} - Q_{AB} - Q_C \right) \tag{13}$$

or, from the chemisorbed state [cf. eq. (8)],

$$\Delta E^*_{f,s} = \Delta E^*_{(AB)C,s} = \tfrac{1}{2}\left(D + \frac{Q_{AB}Q_C}{Q_{AB}+Q_C} + Q_A + Q_{BC} - Q_{AB} - Q_C \right). \tag{14}$$

For the reversed reaction in eq. (11), the activation barrier ΔE_r^* may be calculated as the relevant recombination barrier ΔE^*_{AB-C} from eqs. (9) and (10).

3. Results

Since the BOC-MP method can explicitly treat only mono- and dicoordinated adsorbates, our analysis will be limited to C_1- and C_2-hydrocarbons and oxygenates. The energetic parameters (the atomic heats of chemisorption Q_A and the total gas-phase bond energies D_{AB}) are shown in table 1, which also lists the calculated values of Q_{AB} and $D_{AB} + Q_{AB}$ for appropriate C_1- and C_2-adsorbates on Cu(111), Pt(111), Ni(111) and Fe(110). For these surfaces and for the elementary steps outlined in fig. 1, the calculated activation barriers ΔE^* are summarized in table 2.

Unlike our earlier BOC-MP analyses of the methanation reaction $CO + H_2 \rightarrow CH_4 + H_2O$ on Ni(111), Pd(111) and Pt(111) [6a] and the decomposition of C_2H_x species on Fe(110), Ni(111) and Pt(111) [7a], the present work makes use of the refined BOC-MP formalism [5d,6b,7b]. Thus, many values of Q and ΔE^* have been recalculated, including those related to the disproportionation reactions [eqs. (12)–(14)].

We begin with periodic trends in CO dissociation. The dissociation $CO_g \rightarrow C_s + O_s$ from the gas phase CO_g occurs without activation ($\Delta E^*_{CO,g} < 0$) on Fe(110), requires the little barrier of 6 kcal/mol on Ni(111) and the high barriers of 18 and 39 kcal/mol on Pt(111) and Cu(111), respectively. Judging by the activation barriers of two possible routes to carbidic carbon, $CO_s \rightarrow C_s + O_s$ versus $CO_s + H_s \rightarrow C_s + OH_s$, the presence of H_s further facilitates the dissociation of chemisorbed CO_s on Fe(110) and Ni(111) but is of no help on Pt(111) and Cu(111). We conclude that the dissociation of CO is nonactivated on Fe and easy on Ni but rather difficult on Pt and practically impossible on Cu.

The nonactivated dissociation of CO on Fe surfaces should lead to high coverage θ_C of carbidic carbon (and oxygen), which, in turn, should decrease the values of Q_C (and Q_O) and Q_{CO}. The BOC-MP method allows one to make such coverage-dependent estimates [5a]. Table 3 compares the values of Q_X (X =

Table 1
Heats of chemisorption (Q) and total bond energies in the gas phase (D) and chemisorbed ($D+Q$) states on Cu(111), Pt(111), Ni(111), and Fe(110) [a]

Adsorbate	D	Cu		Pt		Ni		Fe	
		Q	$D+Q$	Q	$D+Q$	Q	$D+Q$	Q	$D+Q$
H		56	56	61	61	63	63	66	66
O		103	103	85	85	115	115	125	125
C [b]		120	120	150	150	171	171	200	200
CH	81	72	153	97	178	116	197	142	223
CH_2	183	48	231	68	251	83	266	104	287
CH_3	293	26	319	38	331	48	341	62	355
CH_4	398	5	403	6	404	6	404	7	405
OH	102	52	154	39	141	61	163	69	171
H_2O	220	14	234	10	230	17	237	19	239
CO	257	12	269	32	289	27	284	36	293
CH_3CO	565	27	592	40	605	50	615	66	631
CH_3CHO	651	16	667	11	662	19	670	22	673
CH_3CH_2O	668	54	722	41	709	64	732	72	740
CH_3CH_2OH	771	15	786	11	782	18	789	21	792
CHCH	392	9	401	14	406	18	410	25	417
CH_2CH	421	40	461	44	465	55	476	71	492
CH_2CH_2	538	8	546	12	550	15	553	20	558
CH_3C	376	71	447	97	473	115	491	141	517
CH_3CH	466	49	515	70	536	85	551	1097	573
CH_3CH_2	576	26	602	39	615	49	625	64	640
CH_3CH_3	674	4	678	5	679	5	679	6	680

[a] The experimental values of Q_X (X = H, O, CO) and D_{AB} from (ref. [5d]). The calculated values Q_{AB} via eqs. (2)–(5). All energies in kcal/mol.
[b] The experimental value of Q_C is known only for Ni(111). For the other surfaces, the values of Q_C were extrapolated (rf. [5d]).

C, O, CO) for a clean Fe(100) surface with those for the experimentally found Fe(100)–$c(2\times2)$C,O structure [8] corresponding to $\theta_{C,O} = 1/2$. For this high coverage, the calculated values of Q_C, Q_O, and Q_{CO} are 178, 82, and 20 kcal/mol, respectively [5d], leading to $\Delta E^*_{CO,g} = 16$ kcal/mol [cf. eq. (7)]. From tables 1 and 2, we conclude that the values of Q_X and $\Delta E^*_{CO,g}$ on carbided Fe surfaces will resemble those on metallic surfaces much less active than metallic Fe, in average close to Pt(111). For this reason, although CO does not directly dissociate on Pt(111) and Cu(111), it makes sense to follow carbon transformations on these surfaces since they can model the FT synthesis on carbided Fe surfaces.

For a given surface, the activation barriers for stepwise hydrogenation of carbidic carbon $C_s \rightarrow CH_s \rightarrow CH_{2,s} \rightarrow CH_{3,s} \rightarrow CH_{4,s}$ decrease with an increase of hydrogen content (with a slight deviation at the last step for Ni and Fe), the periodic trend for each barrier being Fe > Ni > Pt > Cu. The first hydrogenation

Table 2
Activation barriers (in kcal/mol) for forward ΔE_f^* and reversed ΔE_r^* reactions comprising the conceivable elementary steps of the Fischer-Tropsch synthesis on Cu(111), Pt(111), Ni(111), and Fe(110) [a]

Reaction		Cu		Pt		Ni		Fe	
		ΔE_f^*	ΔE_r^*	ΔE_f^*	ΔE_r^*	ΔE_f^*	ΔE_r^*	ΔE_f^*	ΔE_r^*
CO_g	$\rightleftarrows CO_s$	0	12	0	32	0	27	0	36
	$\rightleftarrows C_s + O_s$	39	5	18	6	6	35	−14	68
CO_s	$\rightleftarrows C_s + O_s$	51	5	50	6	33	35	22	54
$CO_s + H_s$	$\rightleftarrows C_{H_s} + OH_s$	51	0	59	0	29	16	20	32
$C_{H_s} + H_s$	$\rightleftarrows CH_s$	31	8	38	5	42	5	46	3
$CH_s + H_s$	$\rightleftarrows CH_{2,s}$	5	27	13	25	17	23	24	22
$CH_{2,s} + H_s$	$\rightleftarrows CH_{3,s}$	0	32	7	26	16	24	19	21
$CH_{3,s} + H_s$	$\rightleftarrows CH_{4,s}$	0	28	6	18	14	14	24	8
	$\rightleftarrows CH_{4,g}$	0	23	6	12	14	8	24	1
$CH_{3,s} + C_s$	$\rightleftarrows CH_3C_s$	7	15	19	11	29	8	43	5
$CH_3C_s + H_s$	$\rightleftarrows CH_3CH_s$	10	22	18	20	22	19	27	17
$CH_{3,s} + CH_s$	$\rightleftarrows CH_3CH_s$	0	43	0	27	10	23	24	19
$CH_3CH_s + H_s$	$\rightleftarrows CH_3CH_{2,s}$	0	31	7	25	13	24	20	21
$CH_{3,s} + CH_{2,s}$	$\rightleftarrows CH_3CH_{2,s}$	0	52	0	33	6	24	20	18
	$\rightleftarrows CH_2CH_{2,s} + H_s$	0	52	0	29	11	20	28	10
$CH_{2,s} + CH_{2,s}$	$\rightleftarrows C_2H_{4,s}$	0	84	0	48	11	32	34	32
$CH_{2,s} + CH_s$	$\rightleftarrows CH_2CH_s$	0	77	2	38	18	31	39	21
$CH_2CH_s + H_s$	$\rightleftarrows C_2H_{4,s}$	0	29	1	25	8	22	17	17
	$\rightleftarrows C_2H_{4,g}$	0	21	1	13	8	7	20	−3
$CH_3CH_{2,s}$	$\rightleftarrows C_2H_{4,s} + H_s$	4	4	4	0	11	2	16	0
$CH_3CH_{2,s} + H_s$	$\rightleftarrows CH_3CH_{3,s}$	0	20	10	13	19	10	29	3
	$\rightleftarrows CH_3CH_{3,g}$	0	16	10	8	19	5	32	−3
$CH_{3,s} + CO_s$	$\rightleftarrows CH_3CO_s$	2	6	16	1	14	4	20	3
CH_3CO_s	$\rightleftarrows CH_3C_s + O_s$	42	0	47	0	33	24	28	39
$CH_3CO_s + H_s$	$\rightleftarrows CH_3C_s + OH_s$	47	0	52	0	32	8	28	19
	$\rightleftarrows CH_3CHO_s$	0	19	14	10	18	10	29	5
	$\rightleftarrows CH_3CHO_g$	0	3	15	−1	27	−9	46	−17
$CH_3CHO_s + H_s$	$\rightleftarrows CH_3CH_2O_s$	7	6	14	0	8	7	8	9
$CH_3CH_2O_s$	$\rightleftarrows CH_3CH_{2,s} + O_s$	19	2	18	9	13	21	9	34
$CH_3CH_2O_s + H_s$	$\rightleftarrows CH_3CH_2OH_s$	10	18	18	30	19	13	24	10
	$\rightleftarrows CH_3CH_2OH_g$	10	3	18	19	24	−5	35	−11

[a] The calculated barriers ΔE^* via eqs. (6)–(14) with the parameters (D_{AB}, Q_{AB}, Q_A, Q_B) from table 1.

$C_s + H_s \rightarrow CH_s$ is strongly endothermic on all the surfaces and requires the highest activation barrier (31–46 kcal/mol for the Cu–Fe range) of all the elementary steps of the FT synthesis (cf. table 2). The other hydrogenation steps are typically exothermic, which makes the relevant activation barriers small, particularly on Pt and Cu.

Let us now turn to the C–C chain growth which may occur by insertion of CH_x or CO into the metal–CH_y bond. Consider first the CH_x–CH_y insertion.

Table 3
Dissociation of CO on Fe(100): Coadsorption effects on Q and ΔE^* [a]

Surface	θ_{CO}	Q_C	Q_O	Q_{CO}	$\Delta E^*_{CO,g}$
Fe(100)	0	200 [b]	120 [b]	34 [b]	−11 [d]
Fe(100)-c(2×2)C,O	1/2	178 [c]	82 [c]	20 [c]	16 [d]

[a] All energies in kcal/mol.
[b] Experimental estimates (ref. [5d]).
[c] BOC-MP calculated values (ref. [5d]).
[d] Eq. (6) for $D_{AB} = 257$.

From table 2 it follows that for a given x the smallest insertion activation barrier holds for the metal–CH_3 (metal-alkyl) bond. Furthermore, for a given metal surface, the activation barrier for insertion $CH_{3,s} + CH_{x,s} \rightarrow CH_3CH_{x,s}$ ($x = 0$–2) decreases as x increases. [We ignore the case of $x = 3$, $CH_{3,s} + CH_{3,s} \rightarrow C_2H_{6,s}$. The reason is that in the chemisorbed $CH_3CH_{3,s}$ there are no direct M_n–C interactions but only M_n–H interactions which makes $CH_3CH_{3,s} \rightarrow CH_3CH_{2,s} + H_s$ be the primary dissociation. From the microscopic reversibility arguments, the direct recombination of chemisorbed methyl radicals appears to be rather improbable (unlike that in the gas phase!).] Thus, the smallest barrier corresponds to the insertion of methylene $CH_{2,s}$ leading to the formation of a homological alkyl, namely $CH_{3,s} + CH_{2,s} \rightarrow C_2H_{5,s}$. The important point here is that the barrier rapidly decreases along the series Fe ≫ Ni ≫ Pt ≃ Cu from 20 to 6 and to 0 kcal/mol, respectively. The similar periodic trends are found for the C–C recombinations $CH_{2,s} + CH_{2,s} \rightarrow CH_2\,CH_{2,s}$ and $CH_{2,s} + CH_s \rightarrow CH_2CH_s$.

In principle, the formation of $CH_3CH_{x,s}$ ($x = 1, 2$) can be envisioned to occur according to the following cycle

$$\begin{array}{ccc} CH_3 + CH_{x-1} & \xrightarrow{\text{insertion}} & CH_3CH_{x-1} \\ \Big\downarrow \text{hydrogenation} & & \Big\downarrow \text{hydrogenation} \\ CH_3 + CH_x & \xrightarrow[\text{insertion}]{} & CH_3CH_x \end{array}$$

namely, the hydrogenation of CH_{x-1} followed by insertion of CH_x (route A) or the insertion of CH_{x-1} followed by hydrogenation of CH_3CH_{x-1} (route B). As seen from table 2, for a given metal surface, the sums of the activation barriers along both routes prove to be very close. Still, route A seems to be preferred. In particular, route B including the C_s insertion ($x = 1$) on Fe and Ni appears to be unfavorable since the deinsertion $CH_3C_s \rightarrow CH_{3,s} + C_s$ requires much lower barriers than the hydrogenation $CH_3C_s + H_s \rightarrow CH_3CH_s$.

Finally, since for all of the metal surfaces but Cu(111) the activation barrier for the dehydrogenation $C_2H_5 \rightarrow C_2H_4 + H$ is smaller than that for the hydrogenation $C_2H_5 + H \rightarrow C_2H_6$, we project that the primary products of the FT synthesis should be α-olefins rather than alkanes.

Consider now the C–C chain growth by insertion of CO into the metal–CH_3 bond. With the exception of Fe(110), this requires the much higher activation barriers than the CH_3–CH_2 insertion, e.g., 14 versus 6 kcal/mol for Ni(111) and 16 versus 0 kcal/mol for Pt(111). Once CH_3CO_s is formed, the C–O bond cleavage, direct or hydrogen-assisted, is much more difficult to achieve than further hydrogenation. For example, on Ni(111) for dissociation reactions $CH_3CO_s \rightarrow CH_3C_s + O_s$ and $CH_3CO_s + H_s \rightarrow CH_3C_s + OH_s$ the activation barriers are 33 and 32 kcal/mol, respectively, whereas for the hydrogenation $CH_3CO_s + H_s \rightarrow CH_3CHO_s$ the barrier is only 18 kcal/mol. As seen from table 2, the acetyl group formed from the CO insertion appears to be a precursor to oxygenates on all the surfaces but Fe(110). The activation barriers for the successive hydrogenation steps $CH_3CO_s \rightarrow CH_3CHO_s \rightarrow CH_3CH_2O_s \rightarrow CH_3CH_2OH_s$ typically decrease along the series Fe > Ni > Pt > Cu.

4. Discussion

The BOC-MP analysis of hydrogenation of CO to form CH_4 and CH_3OH on Pt(111) and Ni(111) has been discussed elsewhere [5d,6], in agreement with experiment. Furthermore, consistent with the projections of the present work, CO has been found to spontaneously dissociate on Fe surfaces such as Fe(111) [9] and Fe(100) [8]. In the latter case, the Fe(100)-$c(2 \times 2)$C,O structure was formed where only molecular (nondissociative) chemisorption of CO has been observed with Q_{CO} = 20–24 kcal/mol [8]. Our conclusion (see above) is that Fe(100)-$c(2 \times 2)$C,O should show the Pt(111)-type behaviour (no dissociation of CO) with Q_{CO} = 20 kcal/mol.

Previously, while analyzing hydrogenation of CO on Ni(111) [6] we have found that there was practically no way to retain the C–O bond and to form CH_3OH, since the activation barriers for the C–O bond cleavage are smaller than those for the hydrogenation $HCO_s \rightarrow CH_3O_s \rightarrow CH_3OH_s$. Moreover, even if CH_3OH_s were formed, its thermal desorption would have been hardly possible, because on Ni(111) we calculate the heat of desorption Q_{CH_3OH} to be distinctly larger (by 5 kcal/mol) than the activation barrier for the O–H bond cleavage [6], in agreement with the LID studies of CH_3OH reactivity on Ni(100) [10]. From table 2 we conclude that metallic Fe is even less suitable for alcohol formation than metallic Ni.

In our previous discussion of C_2H_x decomposition along the periodic series Pt(111) → Ni(111) → Fe(110) [7], we have cited diverse experimental data supporting our conclusions that a rich variety of C_2H_x species can be formed on Pt(111) whereas predominantly C_1H_x species can survive on Fe(110), the Ni(111) and Ru(001) surfaces being intermediate in their propensity to cleave C–H and C–C bonds. Now, these conclusions are expanded over the broader scope of metal surfaces and reactions. Table 2 transparently demonstrates that the peri-

odic trends in the ability of metal surfaces to dissociate chemical bonds and those to recombine the bonds are always opposite. More specifically, the propensity to dissociate CO as well as various hydrocarbons and oxygenates increases in the series Cu < Pt < Ni < Fe but the propensity to propagate the C–C chain (by both CH_2 and CO insertion) and to hydrogenate the adsorbed alkyls and acyls decreases along this series Cu > Pt > Ni > Fe.

An effective FT catalyst should optimize these opposite trends. Furthermore, on an effective catalyst a product should be not only formed but finally desorbed into the gas phase without serious decomposition. The fundamental condition for the latter is that the activation barrier for desorption (equal to the heat of chemisorption Q) has to be smaller than the barrier for decomposition (dissociation, deinsertion, etc.) [5d,10]. From this point of view, clean monometallic surfaces can hardly be optimal FT catalysts. We saw that metallic Fe is excellent for CO dissociation but poor for other intrinsic FT reactions. Moreover, even if hydrocarbons (alkanes or olefins) and oxygenates (aldehydes or alcohols) are somehow formed on Fe(110), they would fail to desorb without decomposition. On the other hand, the Pt(111) and Cu(111) surfaces are practically unable to produce carbidic carbon from CO, so that their superior ability to recombine various fragments and desorb products will remain unrealized.

We conclude that the working FT catalyst should not be clean but modified Fe surfaces, particularly carbided Fe surfaces. This general model conclusion is in agreement with diverse experimental data [1,11,12]. In particular, by using AES and XPS techniques, Krebs et al. [12] have found that the maximum turnover number (TON) for methane is not representative of a clean Fe surface but rather of a surface covered by a large amount of carbidic carbon. Regarding the specific features of the FT synthesis that we have projected, let us restate two of them. First, since of all possible CH_x–CH_y recombinations, the CH_3–CH_2 one has the smallest barrier, we predict that C–C chain growth should occur predominantly via CH_2 insertion into the metal-alkyl bond, in agreement with numerous experimental studies [1,13]. Second, by comparing the activation barriers of hydrogenation versus dehydrogenation of alkyls, we predict that α-olefins rather than alkanes should be primary products of the FT synthesis, again in agreement with experimental observation [1b,14].

The further modification of dissociatively active surfaces to make them effective FT catalysts appears to be formation of bimetallic compositions with nondissociative metals, say Fe (or Co) with Pt or Cu. Indeed, such bimetallic catalysts show prominence not only in producing higher hydrocarbons [1e,11] but also higher alcohols [1e].

Let us stress that within the BOC-MP approach the only experimental parameters used from the realm of chemisorption are atomic binding energies Q_A but the rest are constants–thermodynamic (D_{AB}), structural (n), or numerical (the coefficients obtained by variational procedure). Thus, the calculated values of Q_{AB} for molecular adsorbates listed in table 1 and the values of ΔE^* for various

elementary reactions listed in table 2 are in fact model predictions. Whenever the relevant experimental data are available, the agreement is very encouraging indeed.

5. Conclusions

Although our BOC-MP theoretical analysis deals explicitly with C_1 and C_2 species on well-defined monometallic surfaces, major regularities of the FT synthesis on supported metal catalysts appear to be comprehensible. Both general and specific model projections (the opposite periodic trends in the ability of metal surfaces to dissociate and recombine chemical bonds, the CH_2 insertion as the predominant mechanism of C–C chain growth, α-olefins as the primary FT products, etc.) are consistent with experimental observation. Combined with the earlier successful BOC-MP analyses of various surface reactions [6,7], the present work further strengthens our confidence that the BOC-MP method is accurate enough to be useful.

References

[1] (a) V. Ponec, Catal. Rev. 18 (1978) 151;
(b) A.T. Bell, Catal. Rev. 23 (1981) 23;
(c) P. Biloen and W.M.H. Sachtler, Adv. Catal. 30 (1981) 165;
(d) C.K. Rofer-DePoorter, Chem. Rev. 81 (1981) 447;
(e) C_1 Chemistry: *Proc. 9th Int. Cong. on Catalysis*, eds M.J. Phillips and M. Ternan (The Chemical Institute of Canada, Ottawa, Canada, 1988) Vol. 2.
[2] (a) D.W. Goodman, Acc. Chem. Res. 17 (1984) 194;
(b) P.J. Berlowitz and D.W. Goodman, J. Catal. 108 (1987) 364.
[3] (a) M.A. Vannice, J. Catal. 50 1977) 228;
(b) K. Klier, Adv. Catal. 31 (1982) 241.
[4] M. Ichikawa, A.J. Lang, D.F. Schriver and W.M.H. Sachtler, J. Am. Chem. Soc. 107 (1985) 7216.
[5] (a) E. Shustorovich, Surf. Sci. Rep. 6 (1986) 1;
(b) E. Shustorovich, Acc. Chem. Res. 21 (1988) 183;
(c) E. Shustorovich, J. Mol. Catal. 54 (1989) 301;
(d) E. Shustorovich, Adv. Catal. 37 (1990).
[6] (a) E. Shustorovich and A.T. Bell, J. Catal. 113 (1988) 341;
(b) A.T. Bell and E. Shustorovich, J. Catal. 121 (1990) 1.
[7] (a) E. Shustorovich and A.T. Bell, Surf. Sci. 205 (1988) 492;
(b) A.T. Bell and E. Shustorovich, Surf. Sci., in press.
[8] T.J. Vink, O.L.J. Gijzeman and J.W. Geus, Surf. Sci. 150 (1985) 14.
[9] L. Whitman, L.J. Richter, B.A. Gurney, J.S. Villarubia and W. Ho, J. Chem. Phys. 90 (1989) 2050.
[10] R. Hall, J. Phys. Chem. 91 (1987) 1007.
[11] See, for example, a discussion in: A.F.H. Wieler, G.W. Koebrugge and J.W. Geus, J. Catal. 121 (1990) 375.

[12] H.J. Krebs, H.P. Bonzel and G. Gafner, Surf. Sci. 88 (1979) 269.
[13] R.C. Brady and R. Pettit, J. Am. Chem. Soc. 102 (1980) 6181; 103 (1981) 1287.
[14] See, for example: (a) J.A. Baker and A.T. Bell, J. Catal. 78 (1982) 165;
(b) A.T. Bell, ref. [1e], Vol. 5, p. 134.